Tetrazole-based Inhibitors of the Bacterial Enzyme N-Succinyl-L,L-2,6-Diaminopimelic Acid Desuccinylase as Potential Antibiotics

Thomas DiPuma[1], Emma H. Kelley[1], Teerana Thabthimthong[1], Katherine Konczak[1], Megan Beulke[1], Claire Herbert[1], Thahani Sifna[1], Anna Starus[1], Boguslaw Nocek[2], Ken Olsen[1], Richard Holz[3*], and Daniel P. Becker[1*]

[1]Department of Chemistry and Biochemistry, Loyola University Chicago, 1032 West Sheridan Road, Chicago, IL 60660, USA

[2]Midwest Center for Structural Genomics and Structural Biology Center, Biosciences Division, Argonne National Laboratory, Argonne, Illinois 60439, USA

[3]Department of Chemistry, Colorado School of Mines, 1500 Illinois St., Golden, CO 80401, USA

Abstract

Based on a hit from a high-throughput screen, a series of phenyltetrazole amides were synthesized and assayed for inhibitory potency against DapE from *Haemophilus influenzae* (*Hi*DapE). The inhibitory potency was confirmed but modest, with the most potent analog containing an aminothiazole moiety displayin an IC_{50} = 50.2 ± 5.0 μM. Docking reveals a potential binding mode wherein the amide carbonyl bridges both zinc atoms in the active site, and the tetrazole forms a key hydrogen bond with Asp330.

Introduction

N-Succinyl-L,L-2,6-diaminopimelic acid desuccinylase (DapE) is a bacterial enzyme within the lysine biosynthetic pathway of all Gram-negative and most Gram-positive prokaryotic species including the life-threatening ESKAPE pathogens. As part of global efforts to combat antimicrobial resistance, DapE has emerged as an exciting and promising antibacterial target.[1] DapE is responsible for the production of *m*-DAP and lysine which are ultimately recruited for bacterial peptidoglycan cell wall synthesis. DapE catalyzes the hydrolysis of *N*-succinyl-*L*,*L*-diaminopimelic acid (*L*,*L*-SDAP) to succinic acid and *L*,*L*-diaminopimelate (DAP). DAP acts as the precursor to form *m*-DAP which is then converted to lysine (**Scheme 1**). The enzyme DapE is a promising new antibiotic target due its absence in mammals, thus eliminating the threat of mechanism-based toxicity in humans. Therefore, small molecule inhibitors of DapE may yield antibiotics with a new mechanism of action, of critical importance in fighting antibiotic resistance.

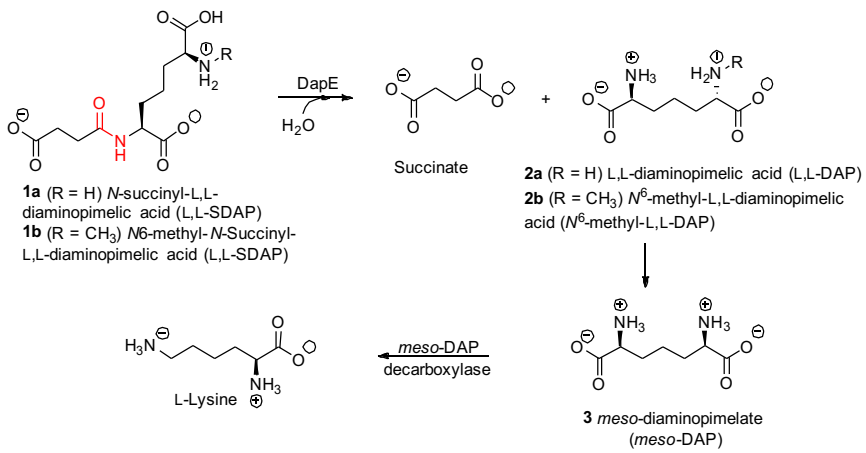

Scheme 1. Enzymatic hydrolysis of L,L-SDAP to succinate and DAP by DapE.

DapE is a di-metallo homodimeric enzyme with catalytic and dimerization domain in each subunit (Fig. 1). The catalytic domain houses the di-nuclear active site consisting of two Zn(II) ions. DapE exists as an open conformation, coaxed into the closed conformation by the binding of substrate for the catalytic cycle that utilizes both catalytic and dimerization domains. We have focused our efforts on understanding the conformational dynamics[2,3] and mechanism of DapE and have sought inhibitors of DapE as potential antibiotics utilizing an assay that we developed that employs the modified substrate **1b** and detection of the enzymatically formed **2b** with ninhydrin.[4] An early directed screen led to the discovery of the ACE inhibitor captopril as the most potent inhibitor of DapE yet reported (IC_{50} = 3.3 μM, Ki = 1.82 ± 0.09 μM, competitive)[5], which was shown bind the active site zinc(II) atoms with its thiol moiety,[6] and has been followed up computationally by Dutta and Mishra toward more potent captopril analogs.[7] An in silico approach toward identification of potential inhibitors of *Helicobacter pylori* DapE was pursued by Das, who identified several dipeptide analogs that were predicted to be inhibitors.[8] Interestingly, Díaz-Sánchez has identified orphenadrine and disulfiram as DapE inhibitors.[9] A high-throughput screen led to the discovery of indoline sulfonamide inhibitors of DapE[10] that we reported previously, as well as a tetrazole thioethers that we now report herein.

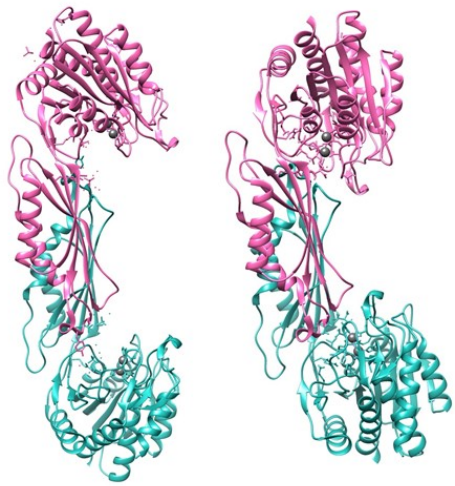

Figure 1. Crystal structures of DapE open and closed forms. (A) Open conformation of *Hi*DapE enzyme (PDB: 5UEJ),[4] (B) closed conformation of *Hi*DapE products-bound structure (PDB:5VO3).[5]

Results and Discussion

A high-throughput screen revealed a tetrazole thioether which we synthesized and explored with a series of tetrazole thioether analogs described herein. Preparation of the phenyltetrazole thioether amides **7a-g** and **8a-g** according to a general method[11] proceeded from the requisite (hetero)aromatic amine which were reacted with chloroacetyl chloride **4a** or 2-chloropropionyl chloride **4b** in methylene chloride at room temperature in the presence of potassium carbonate providing the corresponding α-chloro amide intermediates **5a-g** and **6a-g**. These α-chloro intermediates were then reacted with 1-phenyl-1H-tetrazole-5-thiol in acetone to afford the corresponding phenyl tetrazole thio-linked analogs **7a-g** and **8a-g**. All analogs synthesized were characterized with ^{1}H and ^{13}C NMR as well as high-resolution mass spectrometry (HRMS). All tested derivatives exhibited melting points within a sharp 1-2°C melting range.

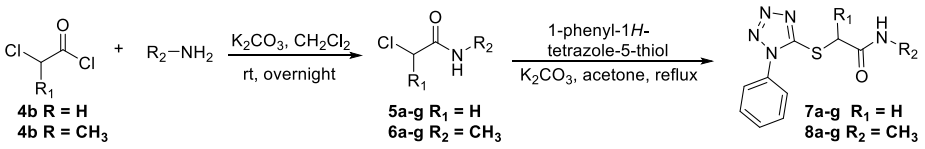

Scheme 2: Synthesis of Tetrazole Analogs **7a-g** and **8a-g**

Inhibitory potencies of tetrazole analogs tested against *Hi*DapE are tabulated in Table 1. Overall, the tetrazole analogs with R_1 = H demonstrated greater potency in comparison to the tetrazole analogs with the R_1 = CH_3 groups. For example, thiazole **7a** exhibits 71.5% inhibition at 100 μM, whereas the

corresponding racemic α-methyl tetrazole analog **8a** inhibits DapE 35.6% at the same concentration, although it is possible that one enantiomer of **8a** is equipotent with **7a** and the distomer of **8a** lacks any potency. This trend of greater potency with R_1 = H is also observed between oxazoles **7b** (49.2%) and **8b** (17.2%), aniline-derived amides **7c** (83.8%) and **8c** (55.4%), and *N*-benzyl derivatives **7g** (61.5%) and **8g** (36.3%), and may be the result of a steric clash of the α-methyl group with the amino acid residues in the active site of DapE. IC_{50} values were determined for the more potent inhibitors, and the most potent tetrazole thioether was 2-aminothiazole derived amide **7a** with an IC_{50} of 50.2 ± 5.0 μM. With respect to druggability, it is noteworthy that these analogs have relatively low MW values ranging from 302-361, and exhibit very low cLogP values ranging from 0.4 to 2.3.

Table 1. Inhibitory potencies of tetrazole thioethers **7a-g** and **8a-g**

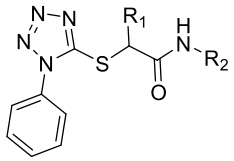

Cmpd	R_1	R_2	M.W. (g/mol)	cLogP Mol/Net	Melting point (°C)	IC_{50} (μM) and/or % Inhibition at 100μM
7a	H		318.4	0.4	214-215	50.2 ± 5.0 71.5%
7b	H		302.3	0.9	179-180	49.2%
7c[12]	H		311.4	1.8	162-164	54.3 ± 6.8 83.8%
7d[13]	H		312.4	1.3	158-160	26.5%
7e	H	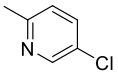	346.8	1.9	183-185	39.5% @75 mM[1]
7f	H		313.3	2.0	154-155	10.2%
7g	H	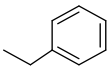	325.4	2.0	103-104	103 ± 6.8 61.5%
8a	CH_3		332.4	0.7	188-190	35.6%
8b	CH_3		316.3	1.2	139-141	17.2%
8c	CH_3		325.4	2.1	123-125	134 ± 3.7 55.4%
8d	CH_3		326.4	1.6	141-143	23.2%
8e	CH_3	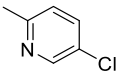	360.8	2.2	116-117	57.3 ± 11.5 71.0%
8f	CH_3		325.4	1.3	137-139	9.7%
8g	CH_3	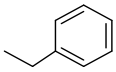	339.4	2.3	74-76	36.3%

[1]Due to lower solubility, **7e** was screened at 75 μM

In order to understand the possible binding modes of the tetrazole analogs to DapE, we performed docking experiments with the most potent analog, thiazole **7a**, with the open form of DapE from *Neisseria meningitidis* (*Nm*DapE). A low energy pose was revealed with very strong interactions illustrated in Figure 2 with the carbonyl oxygen of **7a** is seen to interact with both zinc atoms in a bridging manner, while both N3 and N4 of the tetrazole participate in hydrogen bonds with Arg 330A. In the dinuclear Zn form, each Zn adopts a distorted tetrahedral geometry, where each Zn(II) ion is coordinated by one carboxylate (Glu163 A for Zn1 and Glu135 A for Zn2), and one imidazole (His 67 A for Zn1 and His349 A for Zn2).[3] The interaction of the inhibitor with Arg330 appears to be unique relative to the active site residues that bind products of substrate hydrolysis[2] or the residues that bind the inhibitor captopril.[6]

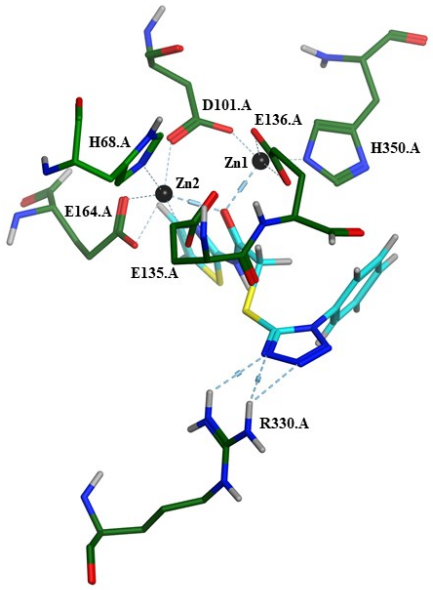

Figure 2. Molecular docking of tetrazole **7a** to the active site of *Nm*DapE PDB 5UEJ

DapE represents a promising new bacterial target toward the discovery of antibiotics with a new mechanism of action, which is critical in combatting morbidity and mortality due to rising global cases of antibiotic-resistant infections. A high-throughput screen revealed a tetrazole thioether lead, which we have confirmed herein and explored initial SAR with the synthesis of a series of analogs resulting in the identification of several phenyl tetrazole amides with double-digit micromolar inhibitory potency. This is a highly druggable scaffold that will serve as a productive lead scaffold for the next generation of DapE inhibitors that are in progress and will be reported in due course.

Declaration of Competing Interest

The authors declare that they have no known competing financial interests or personal relationships that could have appeared to influence the work reported in this paper.

Acknowledgement

Appendix A. Supplementary data

Supplementary data to this article includes full experimental preparations of compounds, characterization data, and IC_{50} curves, and can be found online at….

References

1. Gillner, D. M.; Becker, D. P.; Holz, R. C. *JBIC, J. Biol. Inorg. Chem.* **2013,** *18,* 155.

2. Nocek, B.; Reidl, C.; Starus, A.; Heath, T.; Bienvenue, D.; Osipiuk, J.; Jedrzejczak, R. P.; Joachimiak, A.; Becker, D. P.; Holz, R. C. *Biochemistry (N. Y.)* **2018,** *57,* 574.

3. Kochert, M.; Nocek, B. P.; Habeeb Mohammad, T. S.; Gild, E.; Lovato, K.; Heath, T. K.; Holz, R. C.; Olsen, K. W.; Becker, D. P. *Biochemistry (N. Y.)* **2021,** *60,* 908.

4. Heath, T. K.; Lutz Jr, M. R.; Reidl, C. T.; Guzman, E. R.; Herbert, C. A.; Nocek, B. P.; Holz, R. C.; Olsen, K. W.; Ballicora, M. A.; Becker, D. P. *PloS one* **2018,** *13,* e0196010.

5. Gillner, D.; Armoush, N.; Holz, R. C.; Becker, D. P. *Bioorg. Med. Chem. Lett.* **2009,** *19,* 6350.

6. Starus, A.; Nocek, B.; Bennett, B.; Larrabee, J. A.; Shaw, D. L.; Sae-Lee, W.; Russo, M. T.; Gillner, D. M.; Makowska-Grzyska, M.; Joachimiak, A.; Holz, R. C. *Biochemistry* **2015,** *54,* 4834.

7. Dutta, D.; Mishra, S. *J. Mol. Graph. Model.* **2018,** *84,* 82.

8. Mandal, R. S.; Das, S. *J. Biomol. Struct. Dyn.* **2015,** *33,* 1460.

9. Terrazas-López, M.; Lobo-Galo, N.; Aguirre-Reyes, L. G.; Bustos-Jaimes, I.; Marcos-Víquez, J. Á; González-Segura, L.; Díaz-Sánchez, Á G. *J. Mol. Struct.* **2020,** *1222,* 128928.

10. Reidl, C. T.; Heath, T. K.; Darwish, I.; Torrez, R. M.; Moore, M.; Gild, E.; Nocek, B. P.; Starus, A.; Holz, R. C.; Becker, D. P. *Antibiotics* **2020,** *9,* 595.

11. Kaplancikli, Z. A.; Altintop, M. D.; Turan-Zitouni, G.; Ozdemir, A.; Can, O. D. *Journal of enzyme inhibition and medicinal chemistry* **2012,** *27,* 275.

12. Tai-Bao, W.; Wei, L.; Rong, X.; You-Ming, Z.; Li-Ming, G. *CHINESE JOURNAL OF ORGANIC CHEMISTRY* **2008,** *28,* 99.

13. Kejha, J. *Cesk. Farm.* **1990,** *39,* 294.